Wax Precipitation Modeled with Many Mixed Solid Phases

Robert A Heidemann and Jesper Madsen
Dept. of Chemical and Petroleum Engineering, University of Calgary, Calgary, Alberta T2N 1N4, Canada

Erling H. Stenby and Simon I. Andersen
Dept. of Chemical Engineering, Technical University of Denmark, Lyngby, DK-2800, Denmark

DOI 10.1002/aic.10292
Published online in Wiley InterScience (www.interscience.wiley.com).

The behavior of the Coutinho UNIQUAC model for solid wax phases has been examined. The model can produce as many mixed solid phases as the number of waxy components. In binary mixtures, the solid rich in the lighter component contains little of the heavier component but the second phase shows substantial amounts of the lighter component dissolved in the heavier solid. Calculations have been performed taking into account the recrystallization of the solid alkanes into a second solid form. The Coutinho UNIQUAC model has been used to describe the lower-temperature solid phases. The higher-temperature mixed solid phase has been assumed to be either an ideal solution or to be described by Coutinho's Wilson activity coefficient model. This procedure accounts for more of the known behavior of mixed n-alkane solids. Comparison is also made with results assuming that all of the solid phases, both high-temperature and low-temperature forms, are pure. Model calculations compare well with the data of Pauly et al. for C18 to C30 waxes precipitating from n-decane solutions. © 2004 American Institute of Chemical Engineers *AIChE J,* 51: 298–308, 2005

Introduction

This report deals with a model that describes the precipitation of solid phases (waxes) from hydrocarbon solutions.

The phase behavior in solid alkanes can be complicated, as discussed in detail by Dirand et al. (2002), and much earlier by Turner (1971). The pure *n*-alkanes tend to solidify at their freezing temperatures into a structure that permits molecular rotations (the "rotator" phase). A transition (the so-called order–disorder transition) occurs at a low temperature with a recrystallization into a more rigid structure. Data are available for the *n*-alkane melting temperatures, the temperatures of transition from the rotator phase, and for the associated latent heats (Dirand et al., 2002). For some of the *n*-alkanes there is reported to be a subtle recrystallization within the rotator phase with a small latent heat. This intermediate transition is not so well documented.

The miscibility of *n*-alkanes in binary solid phases depends on the chain lengths of the two molecules and the crystal structure displayed by the pure solids. Dorset (1990) reported on the effect of chain length on solid cosolubility. Some binary pairs show complete miscibility at higher temperatures where the pure solids are in "rotator" phases. This behavior was noted in mixtures when both compounds have an even number of carbon atoms and also when one of the two compounds has an odd number of carbon atoms. When the difference in carbon number is large, the mixtures tend to show true eutectics.

Dirand et al. (2002) summarized the literature on binary *n*-alkane phase behavior. In the low-temperature solid phases, homogeneous solutions can exist in the nearly pure solids. General phase diagrams presented by Dirand et al. show up to three further composition regions of homogeneous solutions at

Correspondence concerning this article should be addressed to R. A. Heidemann at heideman@ucalgary.ca.

low temperature, separated by miscibility gaps. The implication of such diagrams is that three or more crystal structures may appear in the low-temperature waxes.

Models for Solid Precipitation

Many authors have studied the precipitation of waxes. An early contribution of considerable interest was by Butler and MacLeod (1961). They produced a complete model for designing a refinery process for countercurrent fractionation of precipitated *n*-alkane waxes. Their model assumed either that the solid phase was an ideal solution or that the equilibrium ratios between mole fractions in the solid and liquid phases were independent of composition.

A focus of some authors has been the effect of the model used for the liquid phase. Coutinho et al. (1995) examined several liquid-phase activity coefficient models while treating solidification of a single pure compound from solution. One recent comprehensive evaluation of the performance of alternative liquid-phase models in matching solid–liquid equilibria in asymmetric binary *n*-alkane systems is by Polyzou et al. (1999). The binary *n*-alkane solid phases were regarded as ideal solutions in these calculations. The wax formation model of Hansen et al. (1988) also treats the solid as an ideal solution while evaluating a modified Flory model for the liquid.

An alternative to treating the solid as an ideal solution is to assume that the components precipitate as pure solids. This modeling approach has been used by Ungerer et al. (1995) and by Lira-Galeana et al. (1996) and was also contained in the publication by Butler and MacLeod (1961). Pan et al. (1997) and Nichita et al. (2001) separate each heavy pseudo-component into paraffinic, naphthenic, and aromatic parts, each with its own solid–liquid and [only in Nichita et al. (2001)] solid–solid transition points.

Won (1986, 1989) introduced an explicit nonideality into the solid wax phases by using an activity coefficient model of the same type for both the liquid phase and the solid phase. In the 1986 paper, a modified regular solution theory was used with separate solubility parameters for a component in the liquid and in the solid. In the later paper, a Flory–Huggins contribution was added to the activity coefficients. The structure of the model results in an expression for the ratio of equilibrium mole fractions in the solid and liquid phases as a function of temperature and the phase compositions. A separate equation-of-state model was used for the vapor–liquid equilibrium.

Pedersen et al. (1991) reported calculations using a model with the character of the Won model but with a new correlation of the parameters.

Other activity coefficient models that are familiar in describing liquid phases have been adapted for solid *n*-alkane phases by Coutinho and his coinvestigators. Coutinho et al. (1996) and Coutinho and Stenby (1996) presented a parameterization of the Wilson equation to describe the solid *n*-alkanes. This model was used by Lindeloff et al. (1999) to describe high-pressure equilibria in mixtures involving *n*-alkane solids.

Coutinho (1998) noted that the Wilson model is incapable of producing the separation of the solid into mixed phases, as is known to occur in nature. The models proposed by Won (1986, 1989) and Pedersen et al. (1991) could, in principle, require more than one mixed solid phase, but these researchers did not report seeking or finding solid-phase separations in their calculations. In Coutinho (1998), an adaptation of the UNIQUAC equation is proposed. A subsequent paper (Coutinho, 1999) presents alternative methods of fixing parameters in the UNIQUAC model, which has been used to compute wax formation is diesel fuels (Coutinho et al., 2000), cloud points in fuels (Mirante and Coutinho, 2001), and wax formation in crude oils at low pressure (Coutinho and Daridon, 2001).

The model for the low-temperature solid *n*-alkane phases that is used herein is that given in Coutinho (1998). Various models are used for the higher-temperature solids. Coutinho suggested a priori expressions for the molecular size and surface area parameters for the pure *n*-alkanes and for the interaction energies that appear in the UNIQUAC model. The volume parameters r and surface parameters q, in the Coutinho model, are

$$r_n = 0.1C_n + 0.0672 \tag{1}$$

$$q_n = 0.1C_n + 0.1141 \tag{2}$$

where C_n is the carbon number. The energy interaction parameters are evaluated from the heats of sublimation of the pure alkanes. The equations used are

$$\tau_{ij} = \exp[-(\lambda_{ji} - \lambda_{ii})/q_i RT] \tag{3}$$

with

$$\lambda_{ii} = -2(\Delta H_{sub,i} - RT)/Z \tag{4}$$

and the coordination number is assigned a value of $Z = 6$, which is deemed appropriate for the nonrotating orthorhombic crystal structure. The cross-energy parameter λ_{ji} is presumed to be limited by the length of surface contact between molecules of different lengths to the value λ_{ii} for the shorter of the two molecules. That is,

$$\lambda_{ji} = \lambda_{ij} = \lambda_{ii} \tag{5}$$

where molecule i has fewer carbons than molecule j.

The heat of sublimation was taken as the sum of the heat of vaporization, the heat of fusion, and the heat of transition. Heats of vaporization of the *n*-alkanes were obtained from a correlation proposed by Morgan and Kobayashi (1994), which they refer to as PERT2.

The activity coefficient model is expected to be capable of showing phase separations in the solid phase, just as UNIQUAC, when applied to liquid mixtures, can show liquid–liquid phase separations.

Equilibrium between two phases requires the same fugacity for all substances that appear in both phases. For an *n*-alkane in a solid phase, the fugacity is calculated from

$$f_i^s = \gamma_i x_i f_i^{os} \tag{6}$$

with the activity coefficient being obtained from the UNIQUAC model. The standard state fugacity f_i^o is problematic in this expression because it must apply at the phase temperature and pressure.

In our calculations, the standard state fugacity for the pure solid at its melting temperature was calculated from the model used for the liquid, the Soave modification of the Redlich–Kwong equation (SRK; Soave, 1972). The pressure at which the melting temperature was determined (that is, P^o) is presumed to be small (one atmosphere). The effects of temperature and pressure on the standard-state fugacity are calculated from basic identities, assuming equal liquid and solid fugacities at the melting temperature and pressure, to give the result

$$\ln \frac{f_i^{oS1}}{f_i^{oL}} = -\frac{(\Delta \nu_i^{SL})}{RT}(P - P^*) - \frac{(\Delta H_{Mi})}{RT}\left(1 - \frac{T}{T_{Mi}}\right) \quad (7)$$

In Eq. 7, the superscript $S1$ refers to the higher-temperature solid (the rotator phase). The solid for which the Coutinho model applies is the lower-temperature rigid phase. The reference fugacity for this phase is calculated by assuming equal fugacities between the two solid phases at the reference pressure and at the transition temperature, then integrating in the same manner as produced Eq. 7. Eliminating the fugacity of the rotator phase between these two equations yields

$$\ln \frac{f_i^{oS2}}{f_i^{oL}} = -\frac{(\Delta \nu_i^{SL} + \Delta \nu_i^{SS})}{RT}(P - P^*) - \frac{(\Delta H_{Mi})}{RT}\left(1 - \frac{T}{T_{Mi}}\right) - \frac{(\Delta H_{Tri})}{RT}\left(1 - \frac{T}{T_{Tri}}\right) \quad (8)$$

Broadhurst (1962) tabulated melting temperatures T_M, solid–solid transition temperatures T_{Tr}, the heats of melting ΔH_M, and the heats of transition ΔH_{Tr} for the n-alkanes. These values were correlated against carbon number by Lindeloff (1996) and were reported and used by Coutinho (1998). These correlations, attributed to Lindeloff, are used in this work. Although the n-alkanes with odd and even numbers of carbon atoms were reported by Broadhurst to behave somewhat differently from each other, a single correlation was used for all.

The solid–liquid volume change and the solid–solid volume change also appear in the Poynting contributions in Eqs. 7 and 8. These volumes are not always well known and there are issues of compatibility with the equation of state that is being used for the liquid reference fugacity. The calculations we are reporting are at atmospheric pressure. When pressure effects are important, we follow a suggestion of Turner (1971) that the contraction in the liquid–solid transition is 10–20% of the liquid volume and that a further contraction of 2–6% occurs in the solid–solid transition.

There are variations on Eqs. 7 and 8. The two equations are necessary only if the solid–solid transitions are considered. Generally, equations equivalent to just one of the two are used. Coutinho and his collaborators used an equation equivalent to Eq. 8. Won (1986) used Eq. 7, but combined the heat of melting and the heat of transition. In Won (1989), however, Eq. 7 was used as written here. Another issue is that the heats of melting and transition, in a strict sense, are temperature functions. Usually, forms of Eqs. 7 and 8 are used that include this temperature dependency. We felt, however, that given the large uncertainties in the basic quantities the simpler equations would be adequate.

It should be pointed out that the reference fugacity is relevant primarily in liquid–solid equilibria and cancels out of the equations when solids described by the same activity coefficient model are considered to be in equilibrium.

Liquid-Phase Model

As mentioned, the SRK equation was used for components in the liquid phase. The critical temperatures, critical pressures, and acentric factors for the n-alkanes were calculated from the correlations recommended by Twu (1984). Twu also correlated critical volumes and these are required for estimation of the equation-of-state interaction parameters. The equation proposed by Chueh and Prausnitz (1967) was used

$$k_{ij} = 1 - \left(\frac{2\nu_{ci}^{1/6}\nu_{cj}^{1/6}}{\nu_{ci}^{1/3} + \nu_{cj}^{1/3}}\right)^n \quad (9)$$

The equation was used with success for paraffin systems by Lindeloff et al. (1999), setting $n = 1$, and we have used this approach.

Note that this approach leaves no liquid-phase parameters free for data fitting when examining liquid–solid equilibria and that the solid-phase models are also completely determined.

Calculation Procedure

The calculation procedure used has been described by Heidemann and Abdel-Ghani (2001) and, in a version that includes chemical reaction equilibria as well as phase equilibria, by Phoenix and Heidemann (1998). The inner loop of the calculation process is an adaptation of a proposal by Michelsen (1994) for solving multiphase mass balance equations for phase compositions and phase amounts given equilibrium ratios (and equilibrium constants in the case of reacting mixtures). The process locates compositions in potential phases and, as implemented, permits looking for even more phases than the number of components.

Results

Binary phase diagram

The results of computations for binary mixtures of C30 and C36 are shown in Figures 1, 2, and 3. These figures were obtained by performing a series of flash calculations with varying temperatures. The mixture composition at the next temperature was taken as the midpoint of the converged equilibrium at the current temperature. A few such sets of calculations are sufficient to define all the phase boundary lines.

Three different approaches to use of the model equations were used. The results in Figure 1 were obtained by ignoring the possibility of a high-temperature (rotator) phase. The results in Figure 2 were obtained by allowing for the presence of a higher-temperature ideal-solution solid phase (the rotator phase) with all activity coefficients equal to unity and with reference fugacities obtained from Eq. 7. The results in Figure 3 were obtained by using the Coutinho–Wilson activity coefficient model for the high-temperature phase. The Coutinho UNIQUAC model was used for the low-temperature solids in all three cases, with the reference fugacities found by use of Eq. 8.

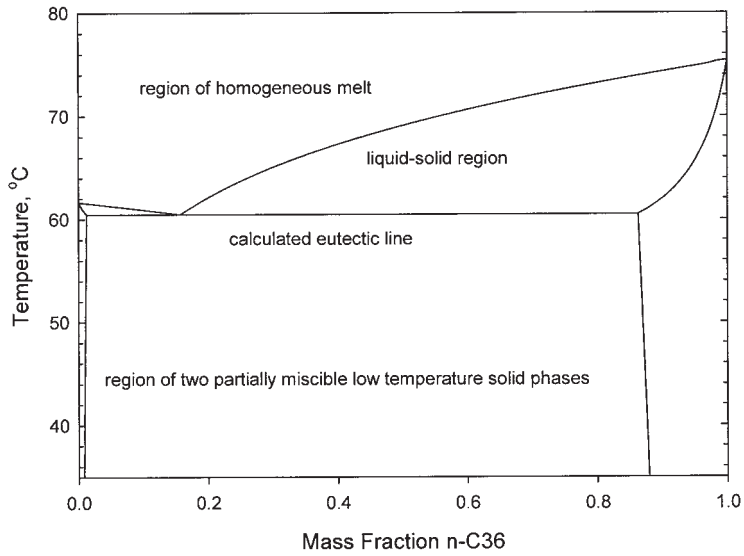

Figure 1. Solid–liquid equilibrium in C30–C36.

UNIQUAC solid phases only.

It is seen in all three figures that the UNIQUAC model requires a solid–solid phase separation in this mixture at sufficiently low temperatures. The compositions of the equilibrium phases at a given temperature are independent of the models used for the high-temperature phases.

Some data for the C30–C36 binary system are given in Dorset (1990). Additionally, approximate phase diagrams for the two systems with deuterated C30 or with deuterated C36 are presented by Snyder et al. (1994). The latter paper shows more clearly than the first what the phase diagram looks like. The solid–solid phase split at temperatures below a eutectoid is clearly indicated.

In Figure 1, the higher-temperature miscible solid phase is missed and solidification below a eutectic produces the two solid phases. The solidification point for each of the pure alkanes is found at a temperature between the experimental fusion temperature and transition temperature. The figure is not at all like the data.

Figures 2 and 3 are more complete (and qualitatively superior) pictures of the actual phase behavior in this system. Key points from the Dorset (1990) measurements are shown in the two figures.

The pure component fusion temperatures and transition temperatures that are used in the equations for the standard-state fugacities are reproduced in this modeling approach. Note that Dorset's values differ somewhat from those given by Dirand (2002). (The Dirand values were used in the C30–C36 calculations.)

The higher-temperature solid mixtures (in the rotator phase) are completely miscible, as is made clear in Snyder et al.

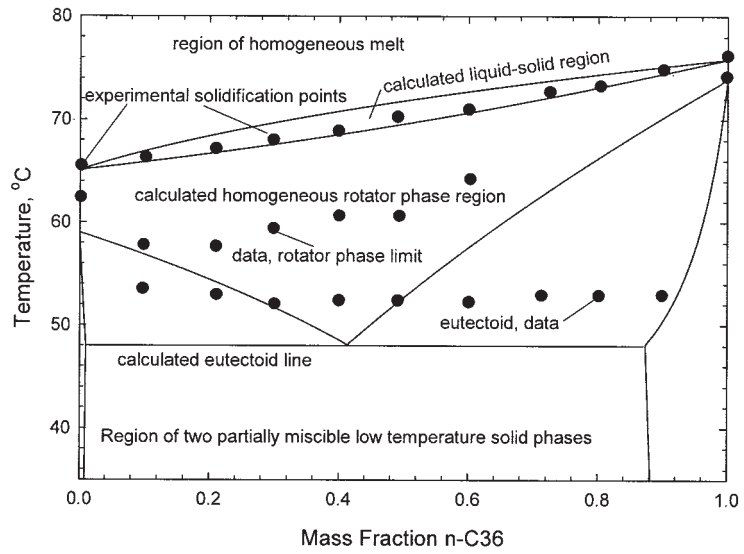

Figure 2. Solid–liquid equilibrium in C30–C36.

An ideal solution rotator phase and low-temperature UNIQUAC solid phases are accounted for.

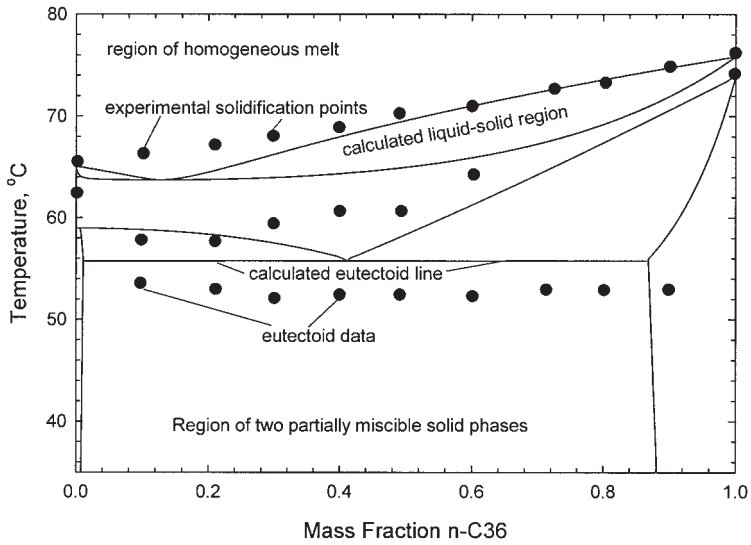

Figure 3. Solid–liquid equilibrium in C30–C36.

A Coutinho–Wilson model rotator phase and low-temperature UNIQUAC solid phases are accounted for. Data shown are taken from Dorset (1990).

(1994). This feature is reproduced by either the ideal solution calculations shown in Figure 2 or the Wilson model calculations shown in Figure 3.

When the ideal solution model is used for the upper phase, the calculated eutectoid temperature is a few degrees lower than is indicated by the Dorset measurements. Calculations with the Wilson model produce a eutectoid temperature closer to the data, but lower.

The solid–solid separations below the eutectoid temperature are asymmetric with only limited solubility of C36 in C30.

A complication in the calculations with the Coutinho–Wilson model is that a "constant-melting" mixture (a solid–liquid analog of the vapor–liquid azeotrope) appears in the equilibrium between the liquid and the high-temperature phase.

These calculations were done without any attempt to fit data. The parameters in the activity coefficient models were used as presented by Coutinho.

Multicomponent mixtures

Additional calculations have been performed on some multicomponent mixtures examined by Pauly et al. (1998). They report detailed liquid–solid phase equilibrium data for systems with *n*-alkanes from C18 to C30 dissolved in *n*-decane. The solid amount and the composition of the equilibrium solid and liquid phases are given. If the solid underwent recrystallization or phase separations, these phenomena would not have been observed.

Pauly et al. (1998) evaluated the performance of six different modeling approaches for solid *n*-alkane precipitation by comparing model predictions with their data. The solid models examined were the first regular solution model of Won (1986), the modified Won model of Pedersen et al. (1991), the ideal solid solution model of Hansen et al. (1988), the Coutinho et al. (1996) Wilson activity coefficient model for the solid, and the Ungerer et al. (1995) model using many pure solid phases. Various models were used for the liquid phases, following the original publications.

None of the models included the possibility of different solids above and below the solid–solid transition temperatures and none looked for solid–solid phase separations. Solid–solid transitions and phase separations can be very important in some systems, as is shown in the C30–C36 phase diagram in Figure 2.

When the Coutinho UNIQUAC model is used for the lower-temperature solids, the Pauly et al. (1998) mixtures show many solid phases, sometimes as many solid phases as there are solid formers. Initially, some calculations were carried out by ignoring the possibility of a higher-temperature miscible solid phase. Table 1 gives details for a typical low- temperature calculation, specifically for the Pauly et al. (1998) mixture B at −1.5°C. At this temperature, the calculations produce 11 different mixed solid phases and a liquid rich in *n*-decane. Table 2 gives details for the same mixture at 16.5°C. At this higher temperature there are six solid phases and a liquid. Typically, the solids rich in the lighter *n*-alkanes dissolve first as the temperature increases.

In the following, some comparisons are made between model calculations and data for mixture C in the study reported by Pauly et al. (1998). The details of the numerical results depend on the approach taken in modeling the higher-temperature solid.

In the first calculations, the possibility of a higher-temperature phase has been ignored. This is essentially the approach taken by Coutinho. We have allowed the *n*-decane solvent to enter the solid phases in this case and in the calculations discussed above for mixture B. The *n*-decane tends to promote solid-phase separations at low temperatures.

Figure 4 shows the fractional precipitation of each of the heavy *n*-alkanes in mixture C over a range of temperatures. Pauly et al. (1998) estimated the temperature at which any solid first appeared in this mixture as 297.35 K. The calculations show the first solid forming at around 300 K. It is interesting that all six of the models examined in the Pauly report result in relatively small errors in this key temperature.

Table 1. Flash Calculations with Pauly et al. Mixture B at −1.5°C*

	Equilibrium Phase											
Fraction	0.7646	0.0347	0.0442	0.021	0.0269	0.0227	0.0161	0.0218	0.0076	0.0211	0.0008	0.0183
n-C10	0.8703	0.013	7E-06	0	0	0	0	0	0	0	0	0
n-C18	0.0601	0.2861	0.0003	0	0	0	0	0	0	0	0	0
n-C19	0.0317	0.5983	0.0523	2E-05	0	0	0	0	0	0	0	0
n-C20	0.0179	0.1023	0.5126	0.0167	4E-05	0	0	0	0	0	0	0
n-C21	0.0094	0.0003	0.4216	0.3740	0.0288	6E-06	0	0	0	0	0	0
n-C22	0.0051	0	0.0131	0.5697	0.4726	0.0152	6E-06	0	0	0	0	0
n-C23	0.0026	0	1E-06	0.0396	0.4825	0.4065	0.0197	1E-06	0	0	0	0
n-C24	0.0014	0	0	7E-06	0.0160	0.5527	0.4621	0.0130	1E-06	0	0	0
n-C25	0.0007	0	0	0	0	0.0255	0.5037	0.4275	0.0146	0	0	0
n-C26	0.0004	0	0	0	0	1E-06	0.0144	0.5418	0.4610	0.0109	0	0
n-C27	0.0002	0	0	0	0	0	0	0.0178	0.5125	0.4434	0.0112	0
n-C28	9E-05	0	0	0	0	0	0	0	0.0120	0.5329	0.4635	0.0151
n-C29	4E-05	0	0	0	0	0	0	0	0	0.0128	0.5155	0.5127
n-C30	2E-05	0	0	0	0	0	0	0	0	0	0.0098	0.4722

*Twelve equilibrium phases are observed, including one liquid and 11 UNIQUAC solids. The fractional amount (in moles) of each phase is in the first row. The liquid composition is in the first column and the compositions of the solid phases follow. Compositions are mole fractions.

Pauly et al. suggest that the onset of precipitation is rather insensitive to the modeling approach and that the variation in the solid-phase composition with temperature is a better measure in differentiating between the model performances. Figure 4 shows a quite reasonable match between the experimental fractional precipitation of the wax formers ranging from C18 to C27 over the range of the data. The Pauly et al. calculations for their mixture A indicated that the Coutinho et al. (1996) and Coutinho and Stenby (1996) Wilson model performed best of those tried in the prediction of fractional precipitation of the lighter wax components. The UNIQUAC model gives results of comparable accuracy.

Figure 5 shows the number of solid phases present at temperatures ranging from 240 K to high temperatures when all the solids have been absorbed into the liquid. The figure presents results for four different modeling approaches. When the UNIQUAC model is used for all solid phases, seven different mixed solids are present over a wide temperature range. Starting at about 270 K, the number of phases is reduced progressively as the temperature is further increased.

Ideal solid solution as the upper phase

As was seen from the model calculations for the C30–C36 system, it can be necessary to include a mixed higher-temperature (rotator) phase to capture the behavior of the solid *n*-alkanes.

Figure 6 was generated by allowing for a mixed ideal solution phase consisting of the higher-temperature forms of the solid *n*-alkanes. Calculations were done for the Pauly et al. mixture C using this method. In these calculations, we excluded the *n*-decane solvent from any solid phases containing the heavier components by setting the equilibrium ratio (K) for *n*-decane to zero. The two possible pure solid *n*-decane phases were allowed for in the calculations. The calculations were initiated at 220 K. At the lowest temperatures, the equilibrium included the pure low-temperature *n*-decane and seven mixed UNIQUAC phases (that is, eight solid phases in all in a mixture with 11 components). At around 227 K the *n*-decane reverted to its higher-temperature form, then melted to form a mixed liquid (still primarily *n*-decane) at around 237 K. Seven UNIQUAC solid phases remained. Figure 5 shows the number of solid phases remaining in the calculation as the temperature continued to increase.

The results shown in Figure 6 are somewhat disappointing in that the lighter components are captured by the ideal solution solid and are removed from the liquid at higher temperatures than is indicated in the data. Pauly et al. (1998) comment that the lighter components do not enter the solid in significant

Table 2. Calculations for the Pauly et al. Mixture B at 16.5°C*

	Phase						
Fraction	0.9399	0.0084	0.0117	0.0059	0.0169	0.0007	0.0166
n-C10	0.7085	0	0	0	0	0	0
n-C18	0.0595	0	0	0	0	0	0
n-C19	0.0504	0	0	0	0	0	0
n-C20	0.0429	0	0	0	0	0	0
n-C21	0.0367	0	0	0	0	0	0
n-C22	0.0315	8E-06	0	0	0	0	0
n-C23	0.0268	0.0253	1E-06	0	0	0	0
n-C24	0.0185	0.5073	0.0105	3E-06	0	0	0
n-C25	0.0107	0.4574	0.3990	0.0210	0	0	0
n-C26	0.0066	0.0099	0.5672	0.5061	0.0095	0	0
n-C27	0.0038	0	0.0234	0.4649	0.4257	0.0148	0
n-C28	0.0022	0	0	0.0080	0.5493	0.4960	0.0141
n-C29	0.0012	0	0	0	0.0155	0.4819	0.5029
n-C30	0.0007	0	0	0	0	0.0074	0.4829

*The results show one liquid phase and 6 UNIQUAC solid phases.

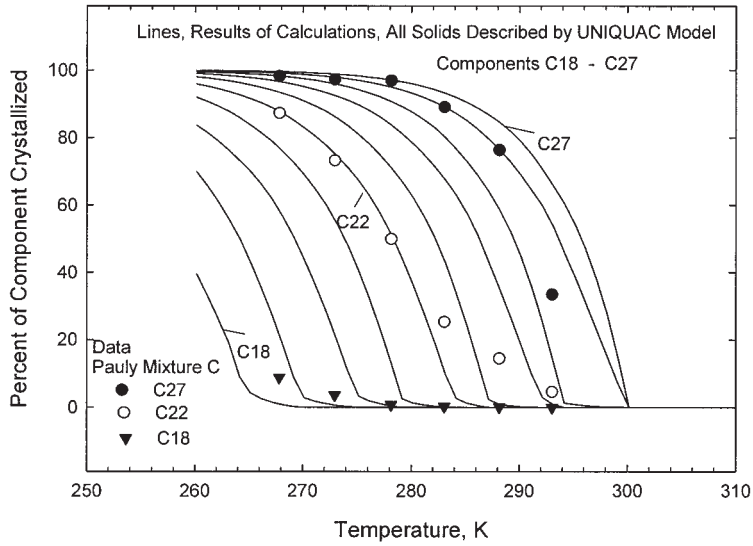

Figure 4. Fractional precipitation of components in the Pauly et al. mixture C, modeled with low-temperature UNIQUAC phases only.

amounts beginning at the first wax precipitation temperature. Our calculations are consistent with results reported by Pauly et al. (1998) in their own experience using an ideal solution model for the solid. The temperature at which the first solid appears is too high and the lighter waxy components enter the solid in significant amounts near this temperature.

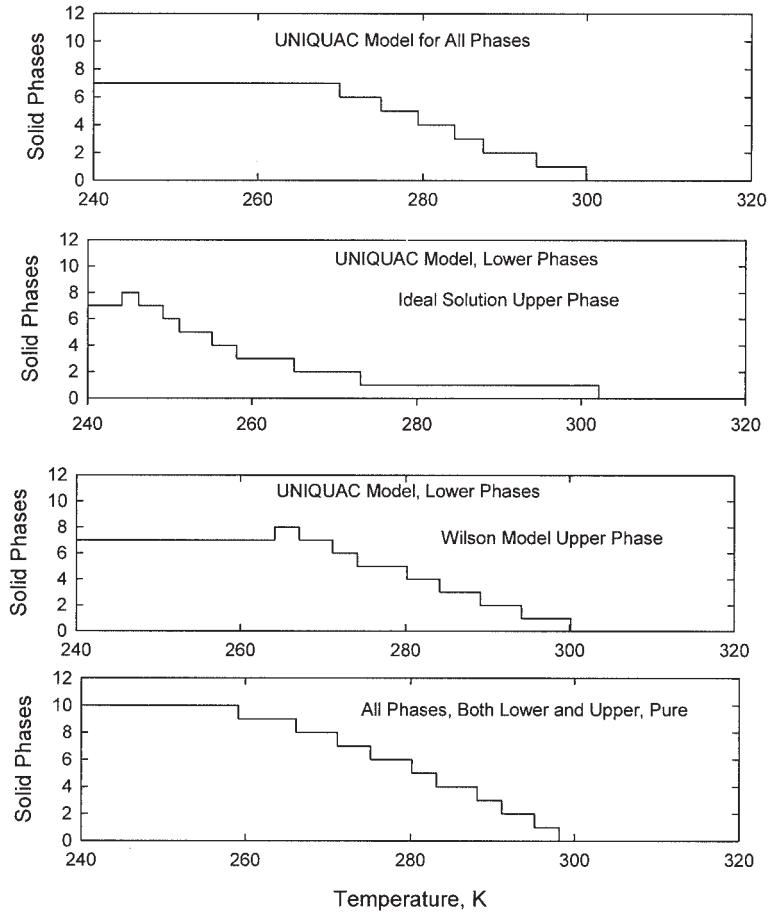

Figure 5. Evolution of the numbers of different solid phases as temperature is increased in four different modeling approaches for the Pauly et al. mixture C.

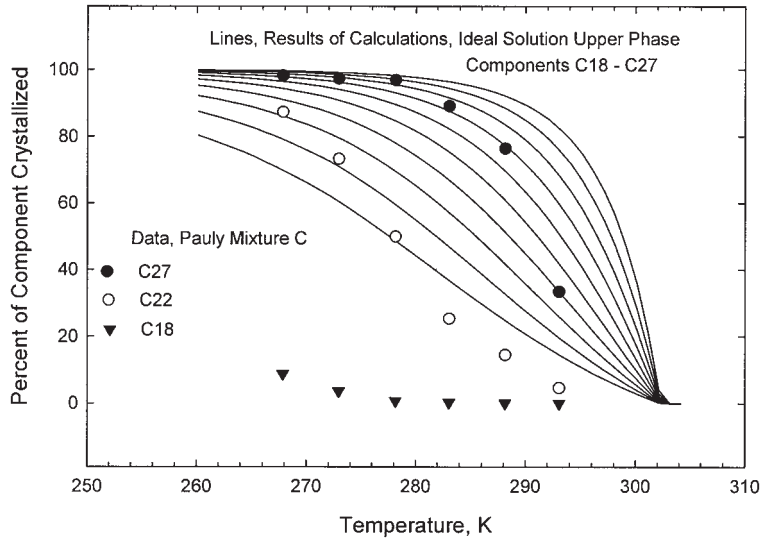

Figure 6. Fractional precipitation of components in the Pauly et al. mixture C, modeled with low-temperature UNIQUAC phases and an ideal solution high-temperature phase.

The UNIQUAC solid phases prove to be irrelevant at temperatures above 275 K in these calculations, given that all have been replaced by the solid ideal solution above this temperature. The ideal solution phase appears at a temperature around 245 K. Briefly there are eight solid phases, seven of which are the UNIQUAC solids. The UNIQUAC solids are absorbed progressively into the ideal solution rotator phase over the subsequent 30 K temperature interval.

Coutinho's Wilson model as the upper phase

As an alternative to treating the higher-temperature mixed solid phase as an ideal solution, calculations have been performed using the Coutinho–Wilson activity coefficient model for this phase. Coutinho's Wilson model is similar to his UNIQUAC model in that the energy parameters were calculated from heats of sublimation using the same reasoning. The Wilson model does not predict any phase separation in the solid and could be thought suitable to represent the higher-temperature phase rotator phase.

In the calculations, the *n*-decane was excluded from the UNIQUAC and Wilson mixed solid phases. However, it was permitted as pure orthorhombic or rotator solids. As the temperature was increased from 220 K, the numbers of phases present and their nature was at first the same as in the previous two cases.

The Wilson solid appeared at about 262.5 K, a much higher temperature than that when the ideal solution phase entered. Over a short temperature range, the model produced eight different solid phases (the seven UNIQUAC phases that persisted from low temperature and the Wilson phase).

UNIQUAC solid phases disappeared in turn as the temperature was increased, in the order of increasing content of heavier components. At 284 K, four phases remained, including a liquid, the Wilson solid, and two heavy UNIQUAC solids.

Surprisingly, the Wilson solid was absorbed next, at about 288.9 K. This phase was relatively richer in the lighter, lower melting, waxy components, which apparently explains its early disappearance.

The last two UNIQUAC solids disappeared at 294.0 and 299.9 K. The final solid was 69.5% C27, 30.4% C26, and 0.1% C25, on a mass basis. These were essentially the same phases as when the rotator phase was not included in the calculations.

Figure 7 shows the uptake of the lighter waxy components into the mixed Wilson phase over the temperature range where the Wilson phase is present. Inclusion of these lighter components in the Wilson solid results in a rather peculiar shape of the curves for the percentage of the C18 to C20 components crystallized. Without the Wilson phase (see Figure 4) the data show more of the C18 component in the solid at lower temperatures. However, with the Wilson upper temperature phase, the calculations show more of the C18 component in the solid than in the data.

All pure solids

The final modeling approach examined was to permit pure solid rotator and orthorhombic phases for each of the components in the mixture, including the *n*-decane solvent. The calculations presumed that there might be a mixed SRK liquid and 22 different solid phases at each temperature. At 240 K, the equilibrium required a liquid phase and pure solid phases of the lower-temperature forms for each of the components heavier than *n*-decane. Solid phases were progressively dissolved or absorbed into the liquid as the temperature increased, until the last solid disappeared at around 297.5 K.

It is interesting to note that 297.5 K is far below the melting temperature and the transition temperature of the heaviest of the components in the mixture. In fact, except for the *n*-decane, the higher-temperature solid (rotator) phase of none of the components entered the calculation.

Figure 8 shows the fractional precipitation of components obtained in this computational approach. Remarkably, the results are not extremely different from those shown in Figures 4 and 7, where the models used were quite different from assum-

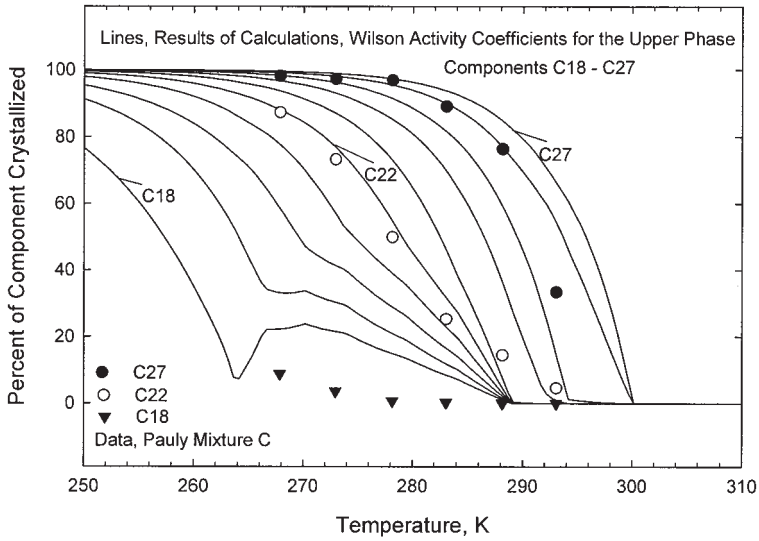

Figure 7. Fractional precipitation of components in the Pauly et al. mixture C, modeled with low-temperature UNIQUAC phases and a Wilson activity coefficient model for the high-temperature phase.

ing pure phases only. The main difference is that solidification of the lighter components begins at lower temperatures than is reflected in the data.

It should be remarked that Ungerer et al. (1995) considered only a single solid-forming component in their calculations. The calculations of Pauly et al. (1998) included many pure solid components but each in only one form, with a reference fugacity calculated from an equation such as Eq. 7 with a combined heat of transition and heat of melting. Lira-Galeana et al. (1996) also considered only one form of each solid and used a modified Eq. 7 for the reference fugacity to account for the temperature dependency of the heat of fusion. On the other hand, Nichita et al. (2001) used an equation such as Eq. 8, which is appropriate for the lower-temperature solid forms.

Comment and Discussion

The calculations reported for the binary C30–C36 system demonstrate the importance of accounting for the phase transitions in the pure solid-forming components when the compositions cover the whole range. A modeling approach that includes the possibility of solid–solid separations in the low-temperature phases and a single homogeneous rotator solid phase is apparently necessary to capture a larger part of the experimental phase behavior, at least where the solid-forming components in the mixture are at sufficiently high concentrations.

The mixtures studied by Pauly et al. (1998), which were perhaps more representative of natural fluids, were relatively

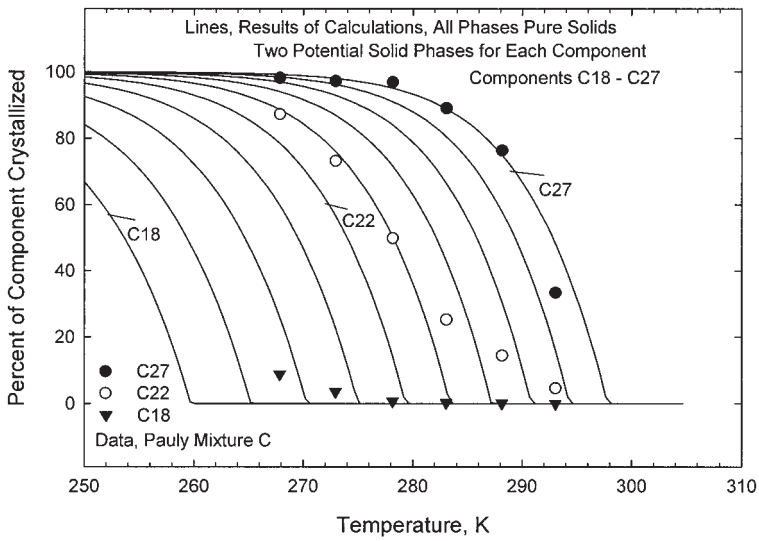

Figure 8. Fractional precipitation of components in the Pauly et al. mixture C, modeled with potentially pure low-temperature phases and pure high-temperature phases for all components.

dilute in the heavy wax-forming constituents. In Coutinho's publications, the solid-phase activity coefficient models are also applied to model solidification from relatively dilute solutions. For those mixtures, the temperatures at which the first solidification occurred were well below the solid–solid transition temperatures of the heaviest components and the high-temperature forms of the solid phases would not be expected.

As noted by Pauly et al., the calculated temperature at which the first solid appeared was insensitive to the modeling approach used, whether the first phase formed was a pure solid, an ideal solution, or a UNIQUAC mixed solid.

The fractional precipitation of the individual solid components was not well described when the upper phase was an ideal solution rotator phase but is reasonably well represented by the UNIQUAC activity coefficient model and by the "all pure solids" model as we implemented it. The pure solids, in our calculations, were found to be of the lower-temperature form.

We think a modeling approach that includes both the rotator phase and the lower-temperature solids (with the possibility of phase separation) is required to anticipate all the possibilities in the phase behavior. In our opinion, the combination of the Coutinho UNIQUAC model for the low-temperature phases and the Coutinho–Wilson model for the higher-temperature solid mixtures provides a reasonable way to treat such fluids.

Petroleum fluids are certainly more complex than the Pauly et al. mixtures. Lira-Galeana et al. (1996) present a discussion of the nature of such fluids and a technique for generating a relatively small number of pseudo-components to represent them. Alternatives to their method of treating these complex mixtures are certainly available, but all ultimately result in the use of pseudo-components. The correlations required to implement the Coutinho models could be used, mechanically, with just this much information.

The Coutinho UNIQUAC model requires computations with possibly many mixed solid phases if it is to be used properly. If a naïve approach is taken and only one UNIQUAC solid is included in the calculations, the results could be erratic. There are potentially many metastable solutions to the equilibrium and mass balance equations that represent local Gibbs free energy minima, including possibly more than one with a single UNIQUAC solid.

The results reported herein were obtained using the formulation and calculation method described in the Appendix. The calculations for the Pauly et al. mixtures were started at a low temperature that resulted in many solid phases and no liquid. Initiation at this temperature included all the pure solids and the liquid of the feed composition. Only when two phases became essentially identical in composition were they combined and the number of phases reduced. Phases of different compositions, even if the amount was zero, were retained in the computations. We trust that all the calculated results presented are correct, in the sense that the global minimum of the Gibbs free energy was reached.

It is certainly simpler to assume only one mixed solid phase in modeling wax precipitation, as has been done by most other researchers. Pedersen and Michelsen (1997) comment further (in a letter to the Editor) that the approach of Lira-Galeana et al. (1996), in which many pure solid phases are anticipated in the wax deposition, is unjustified when dealing with petroleum mixtures described by pseudo-components. No doubt use of the Coutinho UNIQUAC model for such mixtures would be subject to the same reservations. However, the phase separations in low-temperature solid hydrocarbons is clear in the experimental data summarized in Dirand et al. (2002) and a modeling approach that accounts for many mixed low-temperature solid phases and a higher-temperature homogeneous phase seems closer to the known phase behavior of the solid alkanes.

The possibility of detailed comparison with data in multi-solid systems requires additional comment. A remarkable feature of the Coutinho activity coefficient models is that they do not include adjustable parameters. It would, of course, be possible to modify the UNIQUAC or Wilson model energy parameters to fit selected data, but we did not do that. Typically, there is a high sensitivity to parameters in phase separations calculated from solution models, such as UNIQUAC. Others [including Coutinho et al. (1995) and Polyzou et al. (1999)] have noted that the liquid-phase model also has an effect of the matching of data.

Acknowledgments

This research was supported by a grant from the Natural Sciences and Engineering Research Council of Canada.

Literature Cited

Broadhurst, M. G., "Analysis of the Solid Phase Behavior of the Normal Paraffins," *J. Res. Natl. Bur. Stand. A: Phys. Chem.*, **66A**, 241 (1962).

Butler, R. M., and D. M. MacLeod, "Solid–Liquid Equilibria in Wax Crystallization," *Can. J. Chem. Eng.*, **39**, 53 (1961).

Chueh, P. L., Prausnitz, J. M. "Vapor–Liquid Equilibria at High Pressures: Calculation of Partial Molar Volumes in Nonpolar Liquid Mixtures." *AIChE J.*, **13**, 1099 (1967).

Coutinho, J. A. P., "Predictive UNIQUAC: A New Model for the Description of Multiphase Solid–Liquid Equilibria in Complex Hydrocarbon Mixtures," *Ind. Eng. Chem. Res.*, **37**, 4870 (1998).

Coutinho, J. A. P., "Predictive Local Composition Models: NRTL and UNIQUAC and Their Application to Model Solid–Liquid Equilibrium of *n*-Alkanes," *Fluid Phase Equilib.*, **158–160**, 447 (1999).

Coutinho, J. A. P., S. I. Andersen, and E. H. Stenby, "Evaluation of Activity Coefficient Models in Prediction of Alkane Solid–Liquid Equilibria," *Fluid Phase Equilib.*, **103**, 23 (1995).

Coutinho, J. A. P., and J. L. Daridon, "Low-Pressure Modeling of Wax Formation in Crude Oils," *Energy & Fuels*, **15**, 1454 (2001).

Coutinho, J. A. P., C. Dauphin, and J. L. Daridon, "Measurement and Modelling of Wax Formation in Diesel Fuels," *Fuel*, **79**, 606 (2000).

Coutinho, J. A. P., K. Knudsen, S. I. Andersen, and E. H. Stenby, "A Local Composition Model for Paraffinic Solid Solutions," *Chem. Eng. Sci.*, **51**, 3273 (1996).

Coutinho, J. A. P., and E. H. Stenby, "Predictive Local Composition Models for Solid/Liquid Equilibria in *n*-Alkane Systems: Wilson Equation for Multicomponent Systems," *Ind. Eng. Chem. Res.*, **35**, 918 (1996).

Dirand, M., M. Bouroukba, V. Chevallier, D. Petitjean, E. Behar, and V. Ruffier-Meray, "Normal Alkanes, Multialkane Synthetic Model Mixtures, and Real Petroleum Waxes: Crystallographic Structures, Thermodynamic Properties, and Crystallization," *J. Chem. Eng. Data*, **47**, 115 (2002).

Dorset, D. L., "Chain Length and the Cosolubility of *n*-Paraffins in the Solid State," *Macromolecules*, **23**, 623 (1990).

Hansen, J. H., Aa. Fredenslund, K. S. Pedersen, and H. P. Rønningsen, "A Thermodynamic Model for Predicting Wax Formation in Crude Oils," *AIChE J.*, **34**, 1937 (1988).

Heidemann, R. A., and R. M. Abdel-Ghani, "A Ternary System with Five Equilibrium Phases," *Chem. Eng. Sci.*, **56**, 6873 (2001).

Lindeloff, N., "Formation of Solid Phases in Hydrocarbon Mixtures," MS Dissertation, Technical University of Denmark, Lyngby (1996).

Lindeloff, N., S. I. Andersen, E. H. Stenby, and R. A. Heidemann, "Phase-Boundary Calculations in Systems Involving More Than Two Phases,

with Application to Hydrocarbon Mixtures," *Ind. Eng. Chem. Res.*, **38**, 1107 (1999).
Lira-Galeana, C., A. Firoozabadi, and J. M. Prausnitz, "Thermodynamics of Wax Precipitation in Petroleum Mixtures," *AIChE J.*, **42**, 239 (1996).
Michelsen, M. L., "The Isothermal Flash Problem. Part 1. Stability Analysis," *Fluid Phase Equilib.*, **9**, 1 (1982).
Michelsen, M. L., "Calculations of Multiphase Equilibrium," *Comput. Chem. Eng.*, **18**, 545 (1994).
Mirante, F. I. C., and J. A. P. Coutinho, "Cloud Point Prediction of Fuels and Fuel Blends," *Fluid Phase Equilib.*, **180**, 247 (2001).
Morgan, D. L., and R. Kobayashi, "Extension of Pitzer CSP Models for Vapor-Pressures and Heats of Vaporization to Long-Chain Hydrocarbons," *Fluid Phase Equilib.*, **94**, 51 (1994).
Nichita, D. V., L. Goual, and A. Firoozabadi, "Wax Precipitation in Gas Condensate Mixtures," *SPE Prod. Facil.*, **16**, 250 (2001).
Pan, H., A. Firoozabadi, and P. Fotland, "Pressure and Composition Effect on Wax Precipitation: Experimental Data and Model Results," *SPE Prod. Facil.*, **12**, 250 (1997).
Pauly, J., C. Dauphin, and J. L. Daridon, "Liquid–Solid Equilibria in a Decane + Multi-Paraffin System," *Fluid Phase Equilib.*, **149**, 191 (1998).
Pedersen, K. S., and M. L. Michelsen, "Letter to the Editor," *AIChE J.*, **43**, 1373 (1997).
Pedersen, K. S., P. Skovbord, and H. P. Rønningsen, "Wax Precipitation from North Sea Crude Oils. 4. Thermodynamic Modeling," *Energy & Fuels*, **5**, 924 (1991).
Phoenix, A. V., and R. A. Heidemann, "A Non-Ideal Multiphase Chemical Equilibrium Algorithm," *Fluid Phase Equilib.*, **150–151**, 255 (1998).
Polyzou, E. N., P. M. Vlamos, G. M. Dimakos, I. V. Yakounis, and G. M. Kontogeorgis, "Assessment of Activity Coefficient Models for Predicting Solid–Liquid Equilibria of Asymmetric Binary Alkane Systems," *Ind. Eng Chem Res.*, **38**, 316 (1999).
Snyder, R. G., V. H. P. Srivatsavoy, D. A. Cates, H. L. Strauss, J. W. White, and D. L. Dorset, "Hydrogen/Deuterium Isotope Effects on Microphase Separation in Unstable Crystalline Mixtures of Binary *n*-Alkanes," *J. Phys. Chem.*, **98**, 674 (1994).
Soave, G., "Equilibrium Constants from a Modified Redlich–Kwong Equation of State," *Chem. Eng. Sci.*, **27**, 1197 (1972).
Turner, W. R., "Normal Alkanes," *Ind. Eng. Chem. Prod. Res. Dev.*, **10**, 238 (1971).
Twu, C. H., "An Internally Consistent Correlation for Predicting the Critical Properties and Molecular Weights of Petroleum and Coal/Tar Liquids," *Fluid Phase Equilib.*, **16**, 137 (1984).
Ungerer, P., B. Faissat, C. Leibovici, H. Zhou, E. Behar, G. Moracchini, and J. P. Courcy, "High Pressure–High Temperature Reservoir Fluids: Investigation of Synthetic Condensate Gases Containing a Solid Hydrocarbon," *Fluid Phase Equilib.*, **111**, 287 (1995).
Won, K. W., "Thermodynamics for Solid Solution–Liquid–Vapor Equilibria: Wax Phase Formation from Heavy Hydrocarbon Mixtures," *Fluid Phase Equilib.*, **30**, 265 (1986).
Won, K. W., "Thermodynamic Calculation of Cloud Point Temperatures and Wax Phase Compositions of Refined Hydrocarbon Mixtures," *Fluid Phase Equilib.*, **53**, 377 (1989).

Appendix

Multiphase flash calculation process

Equilibrium ratios for each phase, $K_{ij} = X_{ij}/\hat{x}_i$, and the feed composition, z_i, are used to calculate phase amounts, β_j, and phase compositions in an inner loop. Mass balances require

$$X_{ij} = K_{ij} z_i / \sum_j K_{ij} \beta_j \tag{A1}$$

Notably, the reference composition used in defining the equilibrium ratios, $\hat{x}_i$, do not need to be specified. For this reason, no one phase has to be made the reference phase for the calculations and each phase can have its own set of equilibrium ratios.

The equations solved in the inner loop are

$$1 - \sum_i X_{ij} \begin{cases} > 0, & \beta = 0 \\ = 0, & \beta > 0 \end{cases} \tag{A2}$$

Michelsen (1994) showed that these equations are the necessary and sufficient conditions for a constrained minimum of a specific convex function, and thus there is a unique solution. For phases missing, that is with $\beta_j = 0$, the converged value of $-\ln \sum_i X_{ij}$ is equal to the dimensionless "tangent plane distance" in the Michelsen (1982) stability criterion. Mole fractions of all phases, whether present or absent, are obtained by normalizing the X_{ij}. With care, the Newton–Raphson procedure used to solve Eq. A2 can be implemented so that any number of phases can be considered. As is consistent with the requirements of the phase rule, in a mixture with C components, a maximum of C phases with positive phase amounts can be found.

In the outer loop of the procedure, the error in satisfying an equilibrium or minimum tangent plane distance criterion is evaluated through

$$g_{ij} = \left(\ln f_{ij} + \ln \sum_i X_{ij} \right) - \hat{f}_i \tag{A3}$$

where $\hat{f}_i$ is an average fugacity for substance i in the mixture, calculated in the work reported herein as

$$\ln \hat{f}_i = \left[\sum_j \beta_j x_{ij} \ln f_{ij} \right] / z_i \tag{A4}$$

This definition of the average fugacity has two advantages: (1) it avoids use of any one reference phase (which is convenient because any one phase may disappear during the computations) and (2) it allows the possibility that any component may be absent from any one of the phases and only phases present contribute to the value.

Finally, the equilibrium ratios are updated through

$$K_{ij}^{new} = K_{ij}^{old} \exp(g_{ij}) \tag{A5}$$

Note that if one of the equilibrium ratios is defined as zero on initiation of the procedure, it will remain zero throughout.

Manuscript received Oct. 7, 2003, and revision received May 13, 2004.